LETTERS

Temperature-dependent thermal diffusivity of the Earth's crust and implications for magmatism

Alan G. Whittington[1], Anne M. Hofmeister[2] & Peter I. Nabelek[1]

The thermal evolution of planetary crust and lithosphere is largely governed by the rate of heat transfer by conduction[1–3]. The governing physical properties are thermal diffusivity (κ) and conductivity ($k = \kappa\rho C_P$), where ρ denotes density and C_P denotes specific heat capacity at constant pressure. Although for crustal rocks both κ and k decrease above ambient temperature[4,5], most thermal models of the Earth's lithosphere assume constant values for κ ($\sim$1 mm^2 s^{-1}) and/or k ($\sim$3 to 5 W m^{-1} K^{-1})[6,7] owing to the large experimental uncertainties associated with conventional contact methods at high temperatures. Recent advances in laser-flash analysis[8,9] permit accurate ($\pm$2 per cent) measurements on minerals and rocks to geologically relevant temperatures[10]. Here we provide data from laser-flash analysis for three different crustal rock types, showing that κ strongly decreases from 1.5–2.5 mm^2 s^{-1} at ambient conditions, approaching 0.5 mm^2 s^{-1} at mid-crustal temperatures. The latter value is approximately half that commonly assumed, and hot middle to lower crust is therefore a much more effective thermal insulator than previously thought. Above the quartz α–β phase transition, crustal κ is nearly independent of temperature, and similar to that of mantle materials[11]. Calculated values of k indicate that its negative dependence on temperature is smaller than that of κ, owing to the increase of C_P with increasing temperature, but k also diminishes by 50 per cent from the surface to the quartz α–β transition. We present models of lithospheric thermal evolution during continental collision and demonstrate that the temperature dependence of κ and C_P leads to positive feedback between strain heating in shear zones and more efficient thermal insulation, removing the requirement for unusually high radiogenic heat production to achieve crustal melting temperatures. Positive feedback between heating, increased thermal insulation and partial melting is predicted to occur in many tectonic settings, and in both the crust and the mantle, facilitating crustal reworking and planetary differentiation[12].

Thermal diffusivity data for garnet schist, leucogranite and welded rhyolitic ash-flow tuff were acquired at temperatures of up to 1,260 K using laser flash analysis, which isolates the phonon component of heat transfer from radiative transfer and avoids thermal contact losses[13]. Graphite-coated wafers approximately 1-mm thick and 10 mm in diameter are held at some temperature in a furnace. Thermal diffusivity is determined from the time-dependent response of the sample to an additional pulse of heat, supplied by a gadolinium–gallium–garnet laser to the bottom of the sample, which is monitored using an indium antimonide detector above the sample. The leucogranite and rhyolite are homogeneous and isotropic. The schist is anisotropic owing to alternating mica- and quartz-rich layers, so samples were cut parallel and perpendicular to foliation.

Room-temperature ($\sim$298 K) thermal diffusivities ranged from 1.3 to 1.8 mm^2 s^{-1} for the schist, from 1.5 to 2.1 mm^2 s^{-1} for the granite and from 1.8 to 2.2 mm^2 s^{-1} for the rhyolite (Fig. 1). For schist slices cut perpendicular to foliation, heat flow travels parallel to foliation and averages alternating compositional layers; these perpendicular slices yielded values that are intermediate between values for quartz-rich (high-κ) and mica-rich (low-κ) layers sampled by cuts parallel to foliation (when heat flow is across each layer). Variations in κ among different granite and rhyolite samples were also ascribed to differences in the amount of quartz sampled by the laser spot, which is 6 mm in diameter.

For all samples, κ decreased rapidly with increasing temperature, and asymptotically approached a high-temperature limit. Variations among rocks, and among different samples of the same rock, decreased markedly between room temperature and 600 K. Above $\sim$750 K, the κ of the schist samples became very low, probably as a result of differential thermal expansion and cracking along cleavage planes, perhaps accompanied by mica dehydration. The data suggest a break in slope at the quartz α–β transition temperature, followed by a slight, quasi-linear decrease in κ above 846 K. This trend is also observed in quartzites[14].

Data for the two rhyolite samples, two granite samples and the perpendicular schist were fitted by the following equations, which

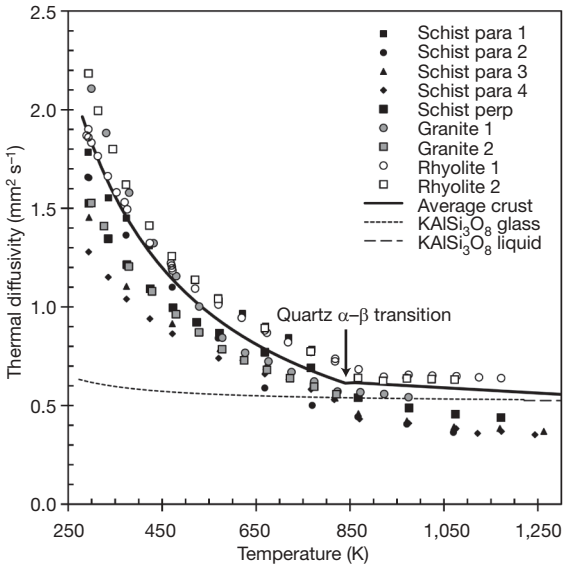

Figure 1 | Thermal diffusivity of crustal rocks as a function of temperature. Data are given in Supplementary Information. Uncertainties are smaller than symbol size in most cases. Curve for average crust calculated using equations (1) and (2) below and above the quartz α–β transition, respectively. Curves for $KAlSi_3O_8$ glass and liquid are from ref. 28. para, parallel; perp, perpendicular.

[1]Department of Geological Sciences, University of Missouri, Columbia, Missouri 65211, USA. [2]Department of Earth and Planetary Sciences, Washington University, St Louis, Missouri 63130, USA.

should be a good estimate of the temperature dependence of thermal diffusivity in the continental crust:

$$\kappa_{\mathrm{crust}}(T<846\mathrm{K}) = 567.3/T - 0.062 \quad (1)$$

$$\kappa_{\mathrm{crust}}(T>846\mathrm{K}) = 0.732 - 0.000135T \quad (2)$$

Here κ is measured in square millimetres per second and T (temperature) is measured in kelvin. Crystalline garnet, pyroxene and olivine all have low average κ values in the range 0.6–0.7 $\mathrm{mm^2\,s^{-1}}$ at upper-mantle temperatures[10,11,15], so any change in κ across the crust–mantle boundary is likely to be minor. Rather, it is within the middle and upper crust that κ changes significantly, by a factor of 3–5.

To calculate thermal conductivity, we derived the following 'bulk crustal' specific heat capacity equations from end-member mineral data[16], on the basis of a mineralogy of 30% quartz, 60% albite, 5% phlogopite and 5% annite:

$$C_{\mathrm{P,crust}}(T<846\mathrm{K}) = 199.50 + 0.0857T - 5.0\times10^{-6}T^{-2} \quad (3)$$

$$C_{\mathrm{P,crust}}(T>846\mathrm{K}) = 229.32 + 0.0323T - 47.9\times10^{-6}T^{-2} \quad (4)$$

Here C_{P} is measured in joules per mole per kelvin, the average molar mass is 221.78 $\mathrm{g\,mol^{-1}}$ and T is measured in kelvin. Although the precise values of C_{P} depend on modal mineralogy, calculated differences in C_{P} among several possible assemblages such as tonalite, granite and schist are <3% at 1,000 K. We assumed a constant density of 2,700 $\mathrm{kg\,m^{-3}}$, because the increase in density due to compression is partly off-set by the decrease due to higher temperatures, and these changes are small in comparison with changes in C_{P} and k.

Calculated values for crustal k decrease with increasing temperature, from ~3.8 $\mathrm{W\,m^{-1}\,K^{-1}}$ at the surface to ~1.9 $\mathrm{W\,m^{-1}\,K^{-1}}$ at the quartz α–β transition, and then decrease only very slightly at higher temperatures (Fig. 2). Our calculations suggest that the k of the lower crust is 25% lower than previous estimates[17], although this depends in part on assumed mineralogy. At 1,000 K, the k of olivine[15] is 3.0 $\mathrm{W\,m^{-1}\,K^{-1}}$, which is 60% higher than that of the crust. Therefore, the middle to lower crust is the most thermally insulating portion of continental lithosphere.

Negative temperature derivatives of κ and k may lead to a positive feedback between temperature increase and heat retention due to decreased thermal diffusivity, in the presence of a heat source. Potential heat sources for continental crust include heat flux from the mantle, radioactive decay, strain heating in deforming rocks and intrusion of mantle-derived basaltic magma. Collisional orogenic belts such as the Himalayas do not derive heat from basalts, yet crustal melting and the generation of leucogranites is a universal feature of such orogens[18]. The mechanism for achieving this has long been debated[19], with most models favouring either unusually high radiogenic heat production in the middle crust[20,21] or strain heating in major shear zones[22–24].

To test the effect of a temperature-dependent κ on the thermal structure of orogenic belts, we used the finite-difference code OROGEN[25] to model the one-dimensional thermal evolution of a doubly thickened crust. The code was modified to incorporate the temperature-dependent κ and C_{P} from equations (1), (2), (3) and (4), and solves the heat flow equation:

$$\frac{\partial T}{\partial t} = \frac{\partial}{\partial z}\kappa\frac{\partial T}{\partial z} + \frac{A_{\mathrm{rad}} + A_{\mathrm{s}}}{\rho C_{\mathrm{P}}} \quad (5)$$

The initial conditions assume stacking of 35-km-thick crust giving the initial sawtooth geotherm. A vertical grid spacing of 250 m was used. The models included radiogenic heat production (A_{rad}) as follows: A_{rad} was 2 $\mathrm{\mu W\,m^{-3}}$ at the surface and reduced exponentially with depth, with a drop-off length of 15 km, to 35 km. Between depths of 35 and 70 km, A_{rad} was constant at 0.2 $\mathrm{\mu W\,m^{-3}}$, and between 70 and 130 km it was constant at 0.02 $\mathrm{\mu W\,m^{-3}}$. For the mantle, the temperature-dependent values of C_{P} and κ were assumed to be those of olivine. Strain heating (A_{s}) occurred within a 3-km-wide shear zone at a depth of 35 km. The rate of strain heating was given by $\tau v/z$ where τ (shear stress) is 30 MPa, v (thrusting velocity) is 3 $\mathrm{cm\,yr^{-1}}$ and z denotes the characteristic width of the shear zone. The effect of strain heating decreased in a Gaussian fashion with distance from the centre of the shear zone (dz) according to $\exp(-dz^2/z^2)$. Temperature was fixed at 1,300 °C at the bottom of 130-km-thick lithosphere. Thrusting was assumed to occur for 40 Myr, followed by 40 Myr of thermal relaxation.

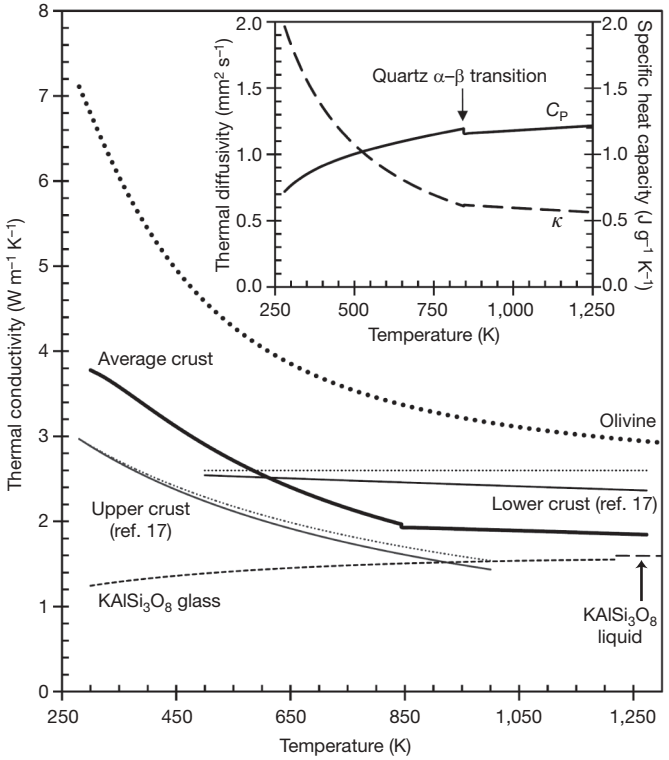

Figure 2 | Thermal conductivity as a function of temperature. Curve for average crust calculated using equations (1), (2), (3) and (4) and a density of 2,700 $\mathrm{kg\,m^{-3}}$. Curve for olivine calculated from ref. 13. Curves for upper and lower crust calculated from ref. 17; dotted curves include pressure dependence of k, assuming a geotherm of 15 $\mathrm{^\circ C\,km^{-1}}$, and solid curves ignore pressure dependence. Curves for $KAlSi_3O_8$ glass and liquid are from ref. 28. Inset, contrasting temperature dependence of thermal diffusivity and specific heat capacity, calculated for average crust from equations (1), (2), (3) and (4).

Models with a constant κ of 1 $\mathrm{mm^2\,s^{-1}}$ (Fig. 3a) show that the schist solidus[18,26] is not reached during 40 Myr of thrusting, and thermal relaxation towards a steady-state geotherm after thrusting does not result in attainment of the temperatures required for crustal melting. Incorporating a temperature-dependent κ accelerates the effect of strain heating because heat does not diffuse efficiently away from the hot shear zone (Fig. 3b). In this model, the schist solidus is reached after 40 Myr. Models with constant radiogenic heat production throughout the lithosphere, for example of 0.1 $\mathrm{\mu W\,m^{-3}}$ (not shown), produce straighter steady-state geotherms, but the effect of a temperature-dependent κ on strain heating is similar.

Our models indicate that the high degree of thermal insulation provided by hot rocks leads to retention of heat generated by strain heating, and that unusually high radiogenic heat production at mid-crustal levels is not required for melting in orogenic belts. We emphasize that the amounts of radiogenic heating used in our models are conservative, and that higher values will lead to earlier and more widespread crustal melting. Moreover, because thermal diffusion through the hot lithospheric mantle and lower crust is slow, there is a more pronounced curvature to the steady-state geotherm with more potential for melting in the lower crust.

Once melting begins, rock strength decreases and the strain-heating mechanism should cease to be effective[27]. However, the κ of $KAlSi_3O_8$

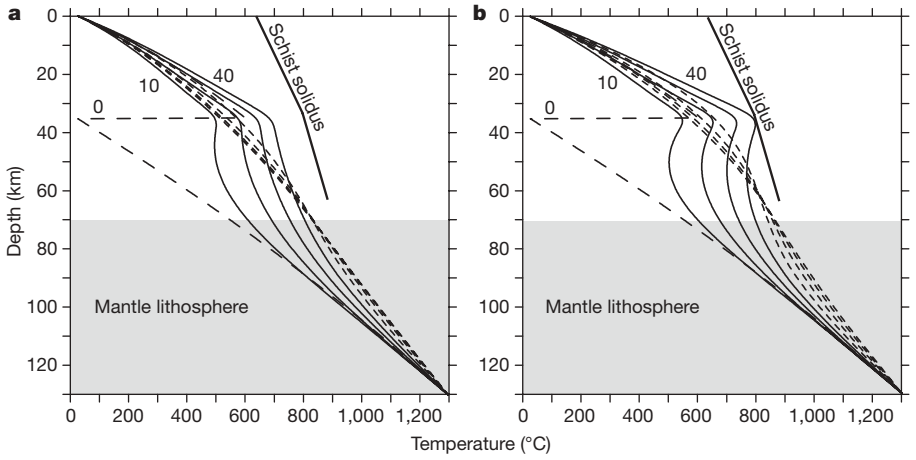

Figure 3 | Thermal models for doubly thickened continental crust with a shear zone at a depth of 35 km. a, Model with a constant κ of 1 mm^2 s^{-1}. Long-dash line is the initial geotherm ($t = 0$), solid lines are geotherms during thrusting at 10-Myr intervals, short-dash lines are relaxation geotherms after cessation of thrusting, also at 10-Myr intervals. Times are indicated in megayears. Schist solidus is from ref. 26. **b**, Model with a temperature-dependent κ, from equations (1) and (2).

glasses and melts is ~20% lower than that of $KAlSi_3O_8$ crystals[28], the k of $KAlSi_3O_8$ glasses and melts is 15–20% lower than that of the bulk crust (Fig. 2), and dissolved water also decreases κ (ref. 29), meaning that hydrous granitic liquids should be particularly efficient insulating materials. The onset of crustal melting may therefore lead to the production of a more insulating layer than the surrounding crust. This positive feedback between melting and thermal insulation may promote increased melt fraction, and allows strain heating to play a significant role in triggering crustal anatexis even though it must become negligible once melting is achieved.

The results of our study pertain to other settings in which partial melting occurs. In both arc and intraplate volcanic settings, basaltic intrusions supply the heat necessary for crustal melting and production of voluminous silicic magmas. Thermal modelling shows that the low thermal diffusivity of hot crust reduces both the long-term flux of mafic magma needed to produce the observed quantities of silicic magma, and the incubation time between the onset of basalt injection and the first eruption of rhyolites[30]. We find values of κ for crustal rocks that are even lower than used in these models, which should result in shorter calculated incubation times. Furthermore, the positive-feedback relations between heating, increased thermal insulation and partial melting will also occur in the mantle, facilitating basaltic magmatism and planetary-scale differentiation.

Received 4 November 2008; accepted 16 January 2009.

1. Thompson, W. The age of the Earth as an abode fitted for life. *Science* **9,** 665–674 (1899).
2. Turcotte, D. L. & Schubert, G. *Geodynamics* 2nd edn, Ch. 4, 132–194 (Cambridge Univ. Press, 2001).
3. Petitjean, S., Rabinowicz, M., Grégoire, M. & Chevrot, S. Differences between Archean and Proterozoic lithospheres: Assessment of the possible major role of thermal conductivity. *Geochem. Geophys. Geosyst.* **7,** doi:10.1029/2005GC001053 (2006).
4. Vosteen, H.-D. & Schellschmidt, R. Influence of temperature on thermal conductivity, thermal capacity and thermal diffusivity for different types of rock. *Phys. Chem. Earth* **28,** 499–509 (2003).
5. Mottaghy, D., Vosteen, H.-D. & Schellschmidt, R. Temperature dependence of the relationship of thermal diffusivity versus thermal conductivity for crystalline rocks. *Int. J. Earth Sci.* **97,** 435–442 (2008).
6. Stein, C. A. & Stein, S. A model for the global variation in oceanic depth and heat flow with lithospheric age. *Nature* **359,** 123–129 (1992).
7. Michaut, C., Jaupart, C. & Bell, D. R. Transient geotherms in Archean continental lithosphere: New constraints on thickness and heat production of the subcontinental lithospheric mantle. *J. Geophys. Res.* **112,** doi:10.1029/2006JB004464 (2007).
8. Degiovanni, A., Andre, S. & Maillet, D. in *Thermal Conductivity 22* (ed. Tong, T. W.) 623–633 (Technomic, 1994).
9. Hofmann, R., Hahn, O., Raether, F., Mehling, H. & Fricke, J. Determination of thermal diffusivity in diathermic materials by the laser-flash technique. *High Temp. High Press.* **29,** 703–710 (1997).
10. Hofmeister, A. M. Thermal diffusivity of garnets to high temperature. *Phys. Chem. Miner.* **33,** 45–62 (2006).
11. Hofmeister, A. M. & Pertermann, M. Thermal diffusivity of clinopyroxenes at elevated temperature. *Eur. J. Mineral.* **20,** 537–549 (2008).
12. Schumacher, S. & Breuer, D. Influence of a variable thermal conductivity on the thermochemical evolution of Mars. *J. Geophys. Res.* **111,** doi:10.1029/2005JE002429 (2006).
13. Hofmeister, A. M., Pertermann, M. & Branlund, J. M. in *Mineral Physics* (ed. Price, G. D.) 543–578 (Elsevier, 2007).
14. Branlund, J. M. & Hofmeister, A. M. Factors affecting heat transfer in natural SiO_2 solids. *Am. Mineral.* **93,** 1620–1629 (2008).
15. Pertermann, M. & Hofmeister, A. M. Thermal diffusivity of olivine-group minerals. *Am. Mineral.* **91,** 1747–1760 (2006).
16. Robie, R. A. & Hemingway, B. S. Thermodynamic properties of minerals and related substances at 298.15 K and 1 bar (10^5 Pascals) pressure and at higher temperatures. *Bull. US Geol. Surv.* **2131,** 1–461 (1995).
17. Chapman, D. S. & Furlong, K. P. in *Continental Lower Crust* (eds Fountain, D. M., Arculus, R. & Kay, R. W.) 179–199 (Elsevier, 1992).
18. Nabelek, P. I. & Liu, M. Petrologic and thermal constraints on the origin of leucogranites in collisional orogens. *Trans. R. Soc. Edinb. Earth Sci.* **95,** 73–85 (2004).
19. Whittington, A. G. & Treloar, P. J. Crustal anatexis and its relation to the exhumation of collisional orogenic belts, with particular reference to the Himalaya. *Mineral. Mag.* **66,** 53–91 (2002).
20. Jamieson, R. A., Beaumont, C., Fullsack, P. & Lee, B. Barrovian regional metamorphism: where's the heat? *Spec. Publ. Geol. Soc. (Lond.)* **138,** 23–51 (1998).
21. Huerta, A. D., Royden, L. H. & Hodges, K. V. The effects of accretion, erosion and radiogenic heating on the metamorphic evolution of collisional orogens. *J. Metamorph. Geol.* **17,** 349–366 (1999).
22. England, P. & Molnar, P. Cause and effect among thrust and normal faulting, anatectic melting and exhumation in the Himalaya. *Spec. Publ. Geol. Soc. (Lond.)* **74,** 401–411 (1993).
23. Harrison, T. M., Grove, M., Lovera, O. M. & Catlos, E. J. A model for the origin of Himalayan anatexis and inverted metamorphism. *J. Geophys. Res.* **103,** 27017–27032 (1998).
24. Nabelek, P. I. & Liu, M. Leucogranites in the Black Hills of South Dakota: The consequence of shear heating during continental collision. *Geology* **27,** 523–526 (1999).
25. Liu, M. & Furlong, K. P. Crustal thickening and Eocene extension in the southeastern Canadian cordillera: Some thermal and mechanical considerations. *Tectonics* **12,** 776–786 (1993).
26. Patiño-Douce, A. E. & Harris, N. Experimental constraints on Himalayan anatexis. *J. Petrol.* **39,** 689–710 (1998).
27. Hartz, E. H. & Podladchikov, Y. Y. Toasting the jelly sandwich: The effect of shear heating on lithospheric geotherms and strength. *Geology* **36,** 331–334 (2008).
28. Pertermann, M., Whittington, A. G., Hofmeister, A. M., Spera, F. J. & Zayak, J. Transport properties of low-sanidine single-crystals, glasses and melts at high temperature. *Contrib. Mineral. Petrol.* **155,** 689–702 (2008).
29. Hofmeister, A. M., Pertermann, M., Branlund, J. M. & Whittington, A. G. Geophysical implications of reduction in thermal conductivity due to hydration. *Geophys. Res. Lett.* **33,** doi:10.1029/2006GL026036 (2006).
30. Annen, C., Blundy, J. D. & Sparks, R. S. J. The genesis of intermediate and silicic magmas in deep crustal hot zones. *J. Petrol.* **47,** 505–539 (2006).

Supplementary Information is linked to the online version of the paper at www.nature.com/nature.

Acknowledgements We thank M. Liu for providing the original version of the program OROGEN. This work was supported by the US National Science Foundation.

Author Information Reprints and permissions information is available at www.nature.com/reprints. Correspondence and requests for materials should be addressed to A.G.W. (whittingtona@missouri.edu).